Electrical Engineering (2006) 89: 41–51
DOI 10.1007/s00202-005-0319-x

ORIGINAL PAPER

M. Vasudevan · R. Arumugam · S. Paramasivam

Development of torque and flux ripple minimization algorithm for direct torque control of induction motor drive

Received: 9 March 2005 / Accepted: 9 June 2005 / Published online: 16 December 2005

Abstract Direct torque control (DTC) is known to produce quick and robust response in AC drives. However, during steady state, notable torque and flux ripple occur. They are reflected in speed estimation, speed response and also in increased noise. This paper proposes a new control algorithm, which provides decoupled control of the torque, and flux with constant inverter switching frequency and a minimum torque and flux ripple. Compared to the other DTC methods, this algorithm is much simpler and has less mathematical operations, and can be implemented on most existing digital drive controllers. Algorithm is based on imposing the flux vector spatial orientation and rotation speed, which defines the unique solution for reference stator voltage. This paper contributes (a) Calculation of stator flux vector, torque and flux increments (b) The position of new stator flux vector determination (c) Calculation of the stator reference voltage (d) comparison of errors of different control strategies. In this paper, computer simulations and experimental results have been discussed for the proposed algorithm.

Keywords Direct torque control · Induction motor · Torque ripple · Flux ripple · Voltage vectors

1 Introduction

Research interest in induction motor sensorless drives has grown significantly over the past few years due to their advantages such as mechanical robustness, simple construction and maintenance. Present efforts are devoted to improve the sensorless operation, especially for low speeds, and to develop robust control strategies [1]. Generally, speed sensorless control strategies of induction motor are classified as follows [4]:

1. Direct field oriented control of induction motor (DFOC)
2. Direct torque control (DTC)

M. Vasudevan (✉) · R. Arumugam · S. Paramasivam
Department of Electrical and Electronics Engineering,
College of Engineering Guindy, Anna University,
Chennai, India
E-mail: vasumame@yahoo.com

High performance electric drives require decoupled torque and flux control. This control is commonly provided through field oriented control (FOC), which is based on decoupling of the torque producing current component and the flux-producing component [2]. FOC drive scheme requires current controllers and coordinate transformations. Current regulated pulse width modulation inverter and inner current loops degrade the dynamic performance in the operating regimes wherein the voltage margin is insufficient for the current control, particularly in the field-weakening region [2,3]. Besides, the existence of the cascaded controller structure, where the flux and torque controllers reside in the 'outer loop' while the current control remains as the inner servo loop, results in a response speed and the resulting bandwidth that are inferior in comparison to the direct control concepts [4].

The problem of decoupling the stator current in a dynamic fashion is avoided by DTC methods [5,18]. DTC provides a very quick and precise torque response without the complex field orientation block and the inner current regulation loop. There have been several DTC based strategies like voltage vector selection strategy using switching table, direct self-control, and deadbeat control strategies. Direct self-control and switching table strategies are very simple and have a rather straightforward implementation, but their switching frequency varies according to the motor speed and the hysteresis bands of torque and flux comparators. In turn, this results in a large torque ripple unless a very short sampling time is provided. DTC based on the deadbeat solution to the machine equations utilize an inverse model to calculate the theoretical voltage vector needed to move the machine torque and stator flux to the desired values in one sample period. This voltage vector is then synthesized over the sample period by the use of space vector modulation (SVM) techniques. However, the calculation of the voltage vector requires the solution of a quadratic equation, which results in two solutions and an optimal solution must be determined. In transient conditions, this quadratic equation has no solution and therefore alternative schemes based on look up tables or torque limitation have to be provided [6–8].

In this paper a novel direct torque algorithm is proposed for the control of the torque and flux of an induction motor, running both in the flux weakening and the constant torque modes and performing well in both the steady and transient states. The algorithm is focused on getting a smooth and ripple-free response of the electromagnetic torque, while reducing parameter dependence and the number of parameters required; preserving a certain simplicity and ease of implementation on most existing digital drive controllers. In principle, the proposed approach relies on the intrinsic properties of an induction motor. Namely, generated torque is proportional to the square of the flux linkage and to the relative speed of the flux vector with respect to the rotor itself. Accelerating the flux rotation relative to the rotor increases torque. In the algorithm, the flux vector angular advancement is divided in to two parts: (a) the angle increment ensuring steady state rotation and (b) the angle increment corresponding to the flux acceleration. The later should be kept at the zero value if no torque changes are required. Positive and negative values of the later angular component correspond to the torque increment and decrement, respectively. In addition to increasing the tangential component of the flux linkage, the radial component is asserted as well, controlling the flux amplitude according to the operating speed and load. In this paper, the algorithm for the calculation of desired flux increments according to desired change in torque and the implementation aspects of voltage command calculation are explained in detail. The computer numerical simulation and the real time experiment support the presented results.

2 Basic induction machine equations

The state-space equations of induction machine in stator fixed reference frame in discrete time form (for small values of the sample time, Δt) are as follows:

$$\frac{\Delta\bar{\psi}_\mathrm{s}}{\Delta t} = \bar{V}_\mathrm{s} - R_\mathrm{s}\bar{I}_\mathrm{s} \tag{1}$$

$$\frac{\Delta\bar{\psi}_\mathrm{r}}{\Delta t} = -R_\mathrm{s}\bar{I}_\mathrm{s} + j\omega\bar{\psi}_\mathrm{r} \tag{2}$$

$$\psi_\mathrm{s} = L_\mathrm{s}\bar{I}_\mathrm{s} + L_\mathrm{m}\bar{I}_\mathrm{r} \tag{3}$$

$$\bar{\psi}_\mathrm{r} = L_\mathrm{r}\bar{I}_\mathrm{r} + L_\mathrm{m}\bar{I}_\mathrm{s} \tag{4}$$

$$T_\mathrm{e} = \frac{3P}{2}\left(\bar{\psi}_\mathrm{s} \times \bar{I}_\mathrm{s}\right) \tag{5}$$

$$\omega_m = \frac{\omega}{P} \tag{6}$$

where $\bar{\psi}_\mathrm{s}$ is the d-and q-axes stator flux complex vector with $\bar{\psi}_\mathrm{s} = \psi_{sd} + j\psi_{sq}$, $\bar{\psi}_\mathrm{r}$ is the d-and q-axes rotor flux complex vector with $\bar{\psi}_\mathrm{r} = \psi_{rd} + j\psi_{rq}$, $\bar{V}_\mathrm{s}$ is the $d-$ and $q-$ axes stator voltage complex vector with $\bar{V}_\mathrm{s} = V_{sd} + jV_{sq}$, $\bar{I}_\mathrm{s}$ is the d-and q-axes stator current complex vector with $\bar{I}_\mathrm{s} = I_{sd} + jI_{sq}$, R_s and R_r are stator and rotor resistance, L_s and L_r are stator and rotor self-inductance, L_m is mutual inductance, T_e is the electromagnetic torque, P is the pole-pair number, ω_m and ω are the mechanical and electrical speed, respectively, and j is the imaginary unit. In the proposed model core losses and saturation are neglected.

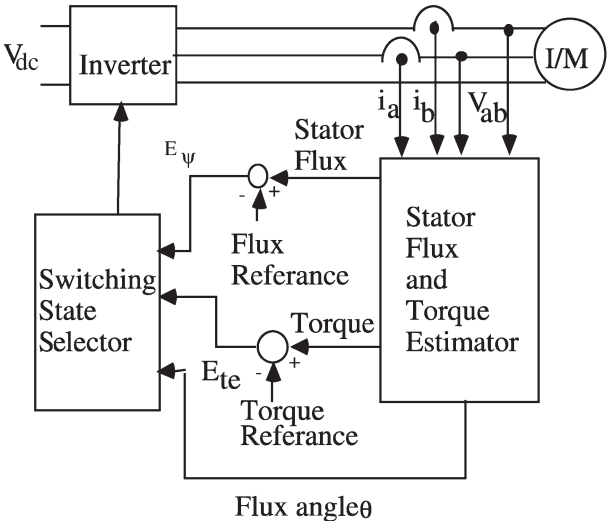

Fig. 1 Schematic of basic direct torque control scheme

3 Direct torque control scheme

The basic schematic of DTC is shown in Fig. 1. In DTC control schemes two discrete equations are given as follows:

$$\Delta T = T^* - T(t_\mathrm{n}), \tag{7}$$

where t_n is the beginning of an arbitrary Δt period, T^* is the reference or command value of torque, and ΔT is desired change in torque, and

$$\Delta\Phi = \Phi^* - \Phi(t_\mathrm{n}), \tag{8}$$

where, Φ^* is the command value of stator flux magnitude, and $\Delta\Phi$ is the desired change in stator flux magnitude.

It is assumed that the torque $T(t_\mathrm{n})$ and stator flux vector $\bar{\psi} = \Phi(t_\mathrm{n})\mathrm{e}^{j\theta(t_\mathrm{n})}$ are correctly estimated, where $\theta(t_\mathrm{n})$ is the stator flux angle to the d-axes in instant t_n.

4 A new direct torque algorithm principle

Stator flux vector $\bar{\psi}_\mathrm{s}$ at instant t_n has the angle $\theta(t_n)$ to the axes fixed to the stator as shown in Fig. 2. Desired flux magnitude Φ^* is represented by a circle centered in the origin with a radius equal to the magnitude of flux reference $\left|\bar{\psi}(t_{n+1})\right| = \Phi^*$. A new DTC algorithm is based on calculating the stator flux vector increment, which will drive torque and flux errors (Eqs. 7 and 8) to zero.

$$\Delta\bar{\psi} = \bar{\psi}_\mathrm{s}(t_{n+1}) - \bar{\psi}(t_n). \tag{9}$$

The desired stator flux vector increment is defined by circle radius and the angle $\Delta\theta$ shown on Fig. 2. So, it is necessary to calculate angle $\Delta\theta$ which depends on the desired

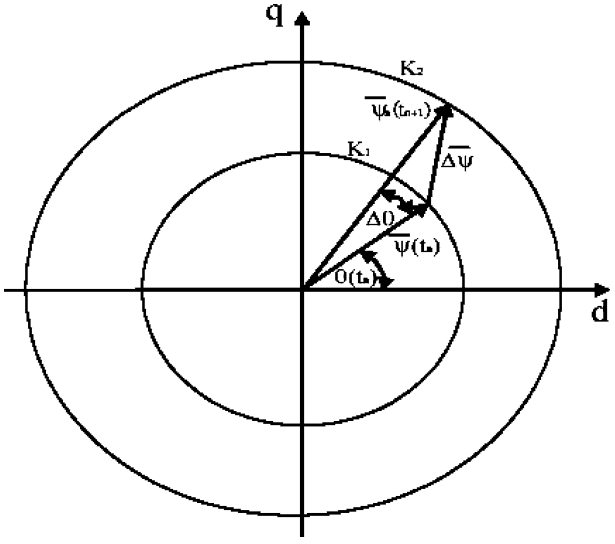

Fig. 2 Definition of stator flux vector increment

changes in torque and flux (Eqs. 7 and 8), and then to calculate stator flux vector increment (Eq. 9). Reference voltage then is:

$$V_s = \frac{\Delta\bar{\psi}}{\Delta t} + R_s\bar{I}_s. \tag{10}$$

It can be seen from Fig. 2 that by increasing the reference flux magnitude, Φ^* the circle radius will be increased and by increasing the reference torque T^* on the same flux level ($\Phi^* = |\overline{\psi}(t_{n+1})| = |\bar{\psi}(t_n)|$) the angle $\Delta\theta$ will be increased.

The equation for developed torque of induction machine given in Eq. (5) can be linearized over the sampling period Δt as:

$$\Delta T = \frac{3}{2}P\left(\bar{\psi}_s \times \Delta\bar{I}_s\right) + \frac{3}{2}P\left(\Delta\bar{\psi}_s \times \bar{I}_s\right) \tag{11}$$

where ΔT is the change in torque, and $\Delta\bar{I}_s$ and $\Delta\bar{\psi}_s$ are the changes in stator current and stator flux. From the inverter driven induction machine in the stationary reference frame, the change in stator current vector $\Delta\bar{I}_s$ is given by:

$$\Delta\overline{I}_s = \frac{\bar{V}^* - \bar{E}}{\sigma L_s}\Delta t, \tag{12}$$

where $\bar{V}^* = \bar{V}_s - R_s\bar{I}_s$, $\sigma = 1 - L_m^2/L_sL_r$ is the leakage coefficient and

$$\bar{E} = j\omega_e\left(\bar{\psi}_s - \sigma L_s\bar{I}_s\right) \tag{13}$$

is the back emf, which is assumed to be sinusoidal with dominant frequency ω_e.

Rotor flux vector and rotor current vector can be rewritten in the meaning of stator quantities by using Eqs. 3 and 4 as:

$$\bar{\psi}_r = \frac{L_r}{L_m}\left(\bar{\psi}_s - \sigma L_s\bar{I}_s\right) \tag{14}$$

$$\bar{I}_r = \frac{1}{L_m}\left(\bar{\psi}_s - L_s\bar{I}_s\right). \tag{15}$$

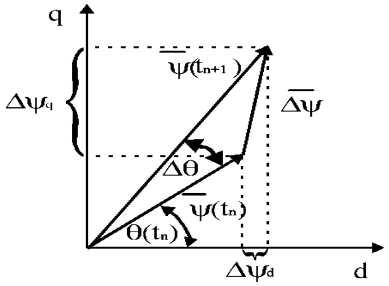

Fig. 3 Projections of stator flux increment vector

Total differential of Eq. 14 is:

$$\Delta\bar{\psi}_r = \frac{L_r}{L_m}\left(\Delta\bar{\psi}_s - \sigma L_s\Delta\bar{I}_s\right) \tag{16}$$

and Eqs. 14–16 have to be substituted in Eq. 2, which gives the expression for stator current as:

$$\bar{I}_s = \frac{\left(1+\sigma T_r^2\omega_s^2\right) + j\left(1-\sigma\right)T_r\omega_s}{L_s\left(1+\sigma^2T_r^2\omega_s^2\right)}\bar{\psi}_s, \tag{17}$$

where $\omega_s = \omega_e - \omega$ is the slip frequency, and $T_r = L_r/R_r$ is the rotor time constant.

Eqs. 13 and 17 have to be substituted in Eq. 12, so the change of stator current will be:

$$\begin{aligned}\Delta\bar{I}_s = {} & \frac{\Delta\bar{\psi}_s}{\sigma L_s} - j\omega_e\Delta t\frac{\left(1-\sigma\right)L_r}{\sigma L_s\left(1+\sigma^2T_r^2\omega_s^2\right)}\bar{\psi}_s \\ & -\omega_e\Delta t\frac{\left(1-\sigma\right)T_r\omega_sL_r}{L_s\left(1+\sigma^2T_r^2\omega_s^2\right)}\bar{\psi}_s\end{aligned} \tag{18}$$

$$\begin{aligned}\bar{\psi}_s \times \Delta\bar{\psi} &= \bar{\psi}_s \times \left[\bar{\psi}_s\left(t_{n+1}\right) - \bar{\psi}_s(t_n)\right] \\ &= \left|\bar{\psi}_s(t_n)\right| \cdot \left|\bar{\psi}_s(t_{n+1})\right| \sin\Delta\theta\end{aligned} \tag{19}$$

$$\Delta\bar{\psi}_s \times j\bar{\psi} = \left|\bar{\psi}_s(t_n)\right| \cdot \left|\bar{\psi}_s(t_{n+1})\right| \cos\Delta\theta - \left|\bar{\psi}_s(t_n)\right|^2 \tag{20}$$

The change in torque can be written by substituting Eqs. 17 and 18 in Eq. 11 and using Eqs. 19 and 20 as:

$$\begin{aligned}\Delta T = {} & \frac{3P\left(1-\sigma\right)\left|\bar{\psi}_s(t_n)\right|}{2\sigma L_s\left(1+\omega_s^2\sigma^2T_r^2\right)}\left[\left|\bar{\psi}\left(t_{n+1}\right)\right|\sin\Delta\theta\right. \\ & \left. -\left|\bar{\psi}_s(t_n)\right|\Delta t\omega_e + \sigma T_r\omega_s\Delta\Phi\right]\end{aligned} \tag{21}$$

For small values of angle $\Delta\theta$,

$$\sin\Delta\theta = \Delta\theta, \tag{22}$$

$$\cos\Delta\theta = 1, \tag{23}$$

so the desired stator flux vector increment angle is:

$$\begin{aligned}\Delta\theta = {} & \frac{2\sigma L_s\left(1+\omega_s^2\sigma^2T_r^2\right)}{3P\left(1-\sigma\right)\left|\bar{\psi}_s(t_n)\right| \cdot \left|\bar{\psi}\left(t_{n+1}\right)\right|}\Delta T \\ & + \frac{\left|\bar{\psi}_s(t_n)\right|}{\left|\bar{\psi}\left(t_{n+1}\right)\right|}\Delta t\omega_e - \frac{\Delta\Phi\sigma T_r\omega_s}{\left|\bar{\psi}\left(t_{n+1}\right)\right|}\end{aligned} \tag{24}$$

It can be seen from Eq. 24 that if there is no change in reference torque ($\Delta T = 0$) and no change in reference flux

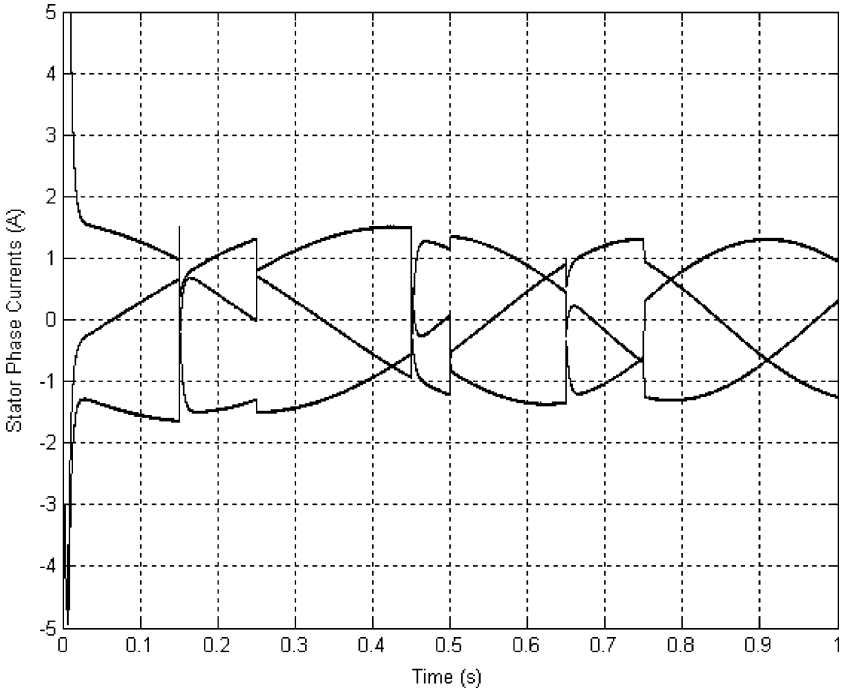

Fig. 4 Simulation results – 3-Phase stator currents of induction motor at 1000 rpm

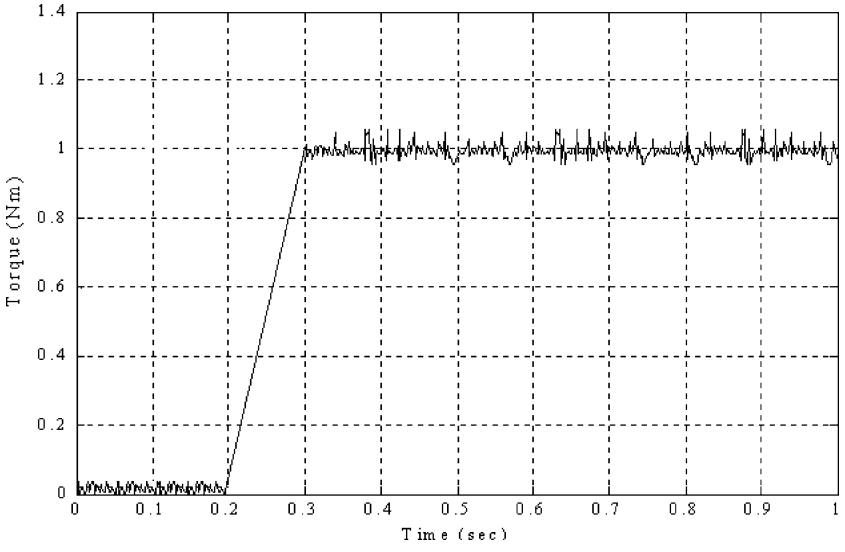

Fig. 5 Simulation results – Torque developed in induction motor using conventional DTC controller at 1000 rpm

($\Delta\Phi = 0$ or $|\bar{\psi}(t_{n+1})| = |\bar{\psi}(t_n)|$) stator flux vector increment angle is $\Delta\theta = \omega_e \Delta t$, which means that the stator flux continues to rotate by synchronous speed. If there is no change in flux ($\Delta\Phi = 0$), and the torque has to be increased, it can be seen from Eq. 24 that the stator flux vector increment angle $\Delta\theta$ has to be increased (and vice versa). If there is a change both in stator flux magnitude and torque, stator flux vector increment angle $\Delta\theta$ can be increased or decreased depending on torque and flux errors (Eqs. 7 and 8).

5 Reference voltage generation

When the desired flux angle movement is determined, the flux projections in stationary dq reference frame from Fig. 3 are:

$$\Delta\psi_d = \left|\bar{\psi}(t_{n+1})\right| \cos(\theta(t_n) + \Delta\theta) - \left|\bar{\psi}(t_n)\right| \cos\theta(t_n) \quad (25)$$

$$\Delta\psi_q = \left|\bar{\psi}(t_{n+1})\right| \sin(\theta(t_n) + \Delta\theta) - \left|\bar{\psi}(t_n)\right| \sin\theta(t_n) \quad (26)$$

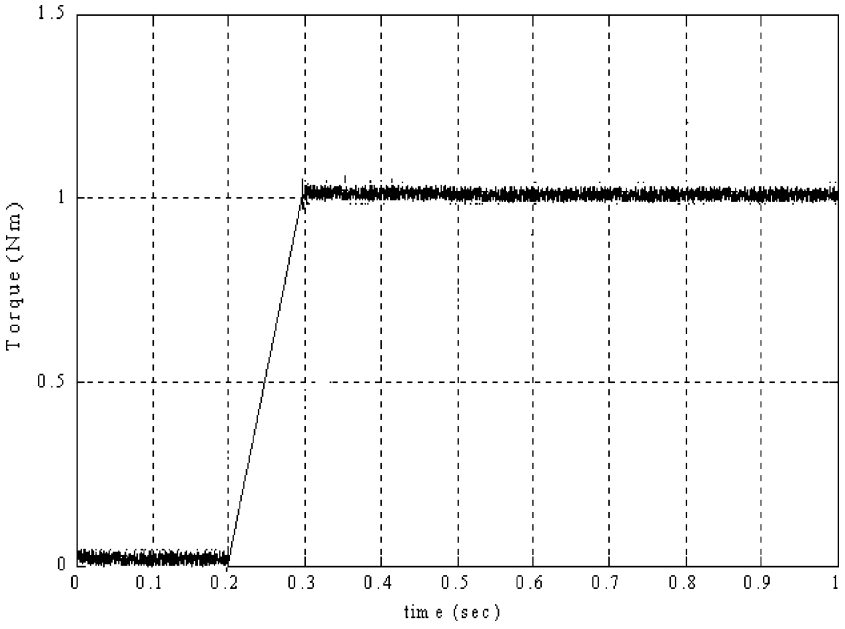

Fig. 6 Simulation results – Torque developed at the application of proposed algorithm of torque and flux ripple minimization at 600 rpm

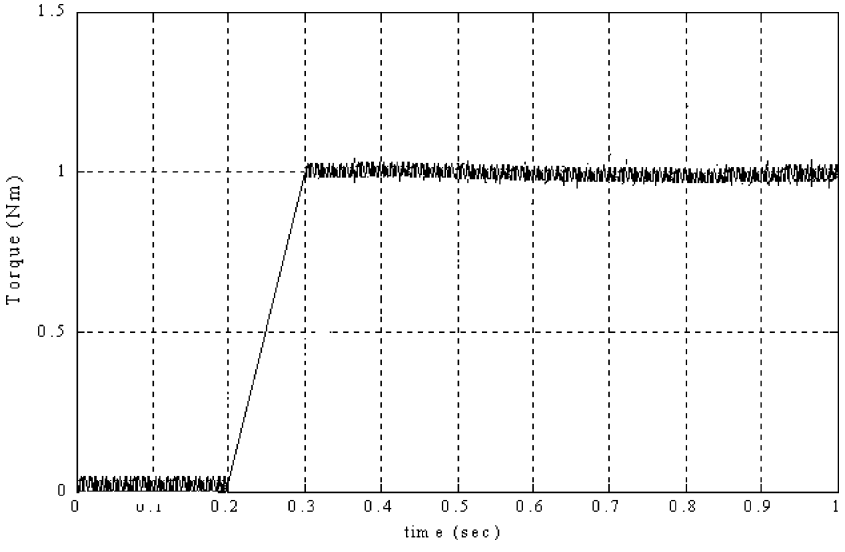

Fig. 7 Simulation results – Torque developed at the application of proposed algorithm of torque and flux ripple minimization at 1000 rpm

Assuming (22–23) and the fact that the stator flux vector components $\psi_d(t_n)$ and $\psi_{\mathrm{q}}(t_n)$ are known, reference voltage components are:

$$V_d^* = \frac{1}{\Delta t \cdot \left|\bar{\psi}(t_n)\right|}\left[\Delta\Phi\psi_d(t_n) - \left|\bar{\psi}(t_{n+1})\right|\psi_q(t_n)\Delta\theta\right] \quad (27)$$

$$V_q^* = \frac{1}{\Delta t \cdot \left|\bar{\psi}(t_n)\right|}\left[\Delta\Phi\psi_q(t_n) + \left|\bar{\psi}(t_{n+1})\right|\psi_d(t_n)\Delta\theta\right] \quad (28)$$

The stator voltage vector reference then is:

$$\bar{V}_{\mathrm{s}} = \left(V_d^* + jV_q^*\right) + R_{\mathrm{s}}\bar{I}_{\mathrm{s}}(t_n) \quad (29)$$

6 Transient conditions

In transient conditions, when the torque and flux errors are too large particularly in field weakening region, the reference voltage will be larger than the available inverter voltage. In that case, the angle $\Delta\theta$ has to be limited, so the reference voltage is lower or equal to the maximum inverter voltage:

$$\left|\bar{V}_{\mathrm{s}}\right| \leq U_{\max}, \quad (30)$$

where $U_{\max}$ is the maximum available inverter voltage.

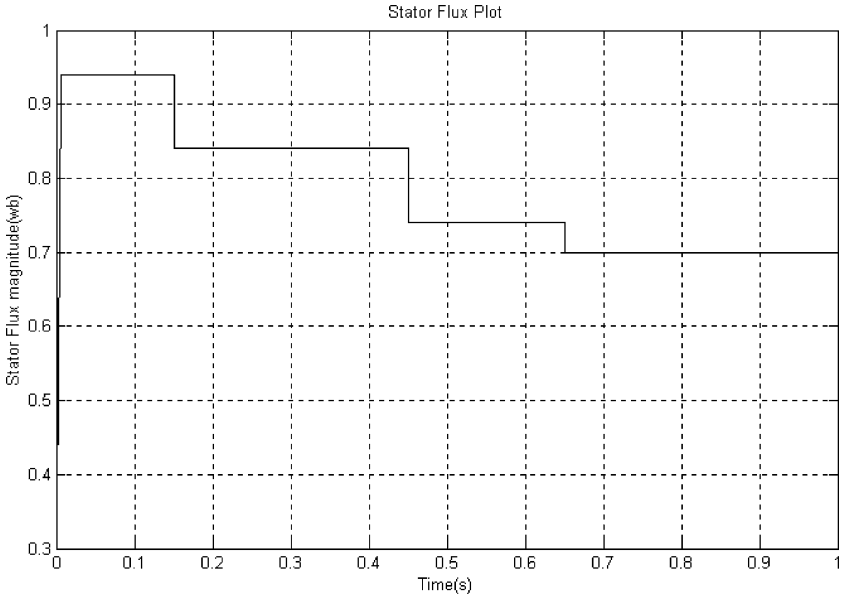

Fig. 8 Simulation results – Magnitude of Stator flux plot at 1000 rpm

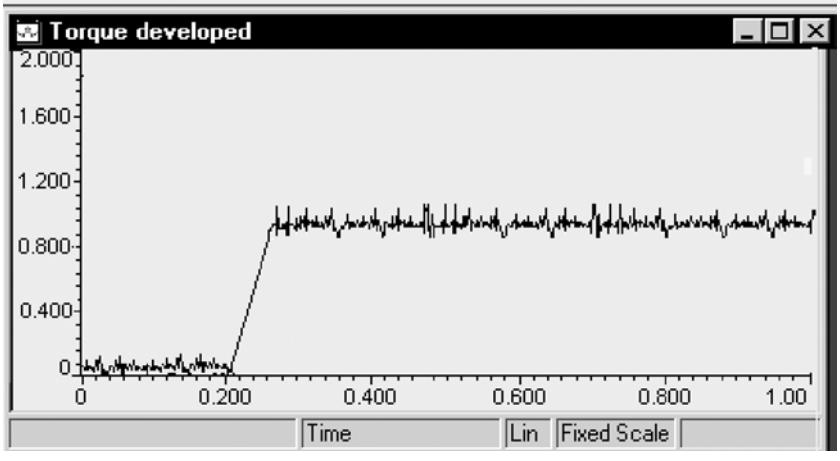

Fig. 9 Experimental results – Torque developed in induction motor using conventional DTC controller at 1000 rpm

Neglecting stator IR voltage drop, and substituting Eqs. 27 and 28 in Eq. 30 maximum angle rotation $\Delta\theta$ allowed is:

$$\Delta\theta \leq \pm\frac{\sqrt{U_{\max}^2(\Delta t)^2 - (\Delta\Phi)^2}}{\left|\bar{\psi}(t_{n+1})\right|}. \tag{31}$$

In this regime direct flux control is enabled, and torque is driven to its reference with the maximum increment possible.

7 Steps of proposed algorithm

Implementation of the proposed algorithm is embodied in the following steps:

1. Determine the state vector, $\underline{x}(\omega_e, \omega_s, \overline{\psi}(t_n), |\bar{\psi}(t_{n+1})|)$ and calculate torque and flux increments, ΔT_e and $\Delta\Phi$ from the estimated values. This step is executed by using Eqs. 7 and 8.
2. Calculate the angle of stator flux adjacent $\Delta\theta = f(\Delta T_e, \Delta\Phi, \underline{x})$ which defines the position of the new stator flux vector $\bar{\psi}(t_{n+1})$ with respect to $\bar{\psi}(t_n)$. This step is executed by eq. 24.
3. Limit the angle $\Delta\theta$ if necessary. This step is executed by using Eq. 31.
4. Calculate the stator flux vector increment $\Delta\bar{\psi}$ using Eqs. 25 and 26.
5. Calculate the stator reference voltage using Eqs. 27, 28, and 29.

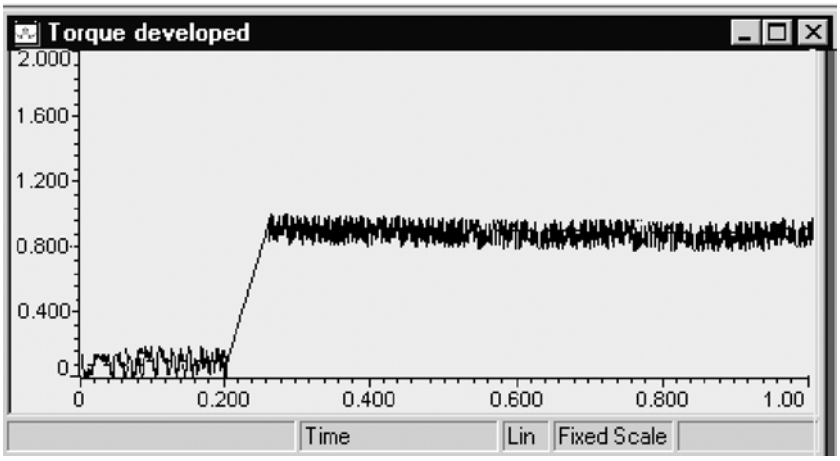

Fig. 10 Experimental results – Torque developed at the application of proposed algorithm of torque and flux ripple minimization at 600 rpm

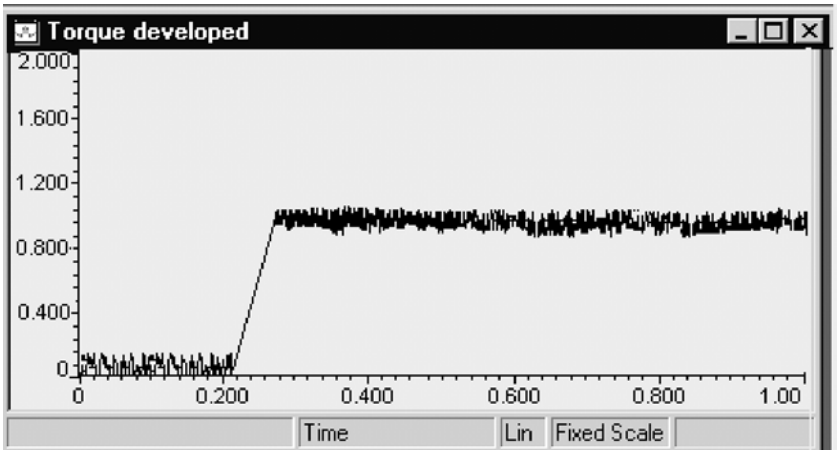

Fig. 11 Experimental results – Torque developed at the application of proposed algorithm of torque and flux ripple minimization at 1000 rpm

8 Results and discussions

Results of computer simulation of induction motor controlled through the proposed algorithm are shown in Figs. 4, 5, 6, 7, and 8. Model is based on Eqs. 1,2,3,4,5, and 6 in state-Space domain without neglecting the saturation, which is modeled by magnetization characteristic. Motor data are given in Appendix. Figure 4 shows the simulation results of 3-phase stator currents of induction motor. It can be seen that the currents are changing their magnitude, frequency, and phase angle due to changes in torque and flux reference. Reference value or command value of torque is 1 Nm, and motor flux is weakened to 0.8 and 0.6 of nominal value. These are taken for both simulation and experiment. Reference or command value of flux is 0.8 wb. Torque developed at 1000 rpm, using conventional DTC controller is shown in Fig. 5. Figures 6 and 7 are torque developed at different speeds such as 600 and 1000 rpm, respectively. Figure 8 shows the magnitude of stator flux in flux weakening region. It can be seen from Figs. 6, 7, and 8 that decoupled control of torque and flux is achieved with minimum torque and flux ripple, and the initial error is minimized in dead-beat manner.

Experimental investigation was focused on the torque and flux controllers using proposed algorithm to minimize the torque and flux ripple. The experimental setup consisted of a three-phase induction motor, IGBT inverter and DSP TMS320LF2407 processor. Inverter is driven by space vector modulation technique with constant 10 kHz switching frequency. Two-phase currents and two-phase voltages were measured from the stator side of the motor. No shaft sensor was used for speed and position feedback. The processor used for experimental work is 16 bit and fixed-point processor. The algorithms are implemented through assembly language coding and results were captured using code composer studio software package. Figure 9 shows the experimental result of torque developed in induction motor using conventional DTC controller. It is observed that both simulation and experimental results are same and torque ripple content is more using conventional DTC algorithm. Initial torque ripple is shown till 0.2 s and enters into transient period. Duration of the transient period is about 0.6 s. From the conventional DTC torque waveform, it is observed that the steady state torque oscillates between 0.88 and to 1.04 Nm. Reference or command torque value is 1 Nm. Figures 10 and 11 show the torque developed

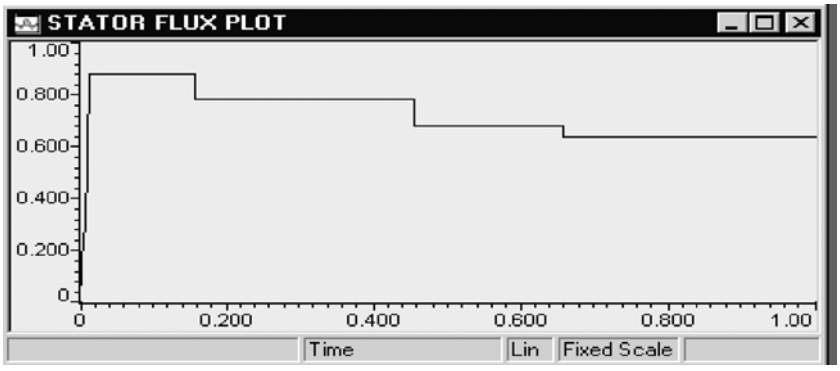

Fig. 12 Experimental results –Stator flux plot at the application of proposed algorithm of torque and flux ripple minimization at 1000 rpm

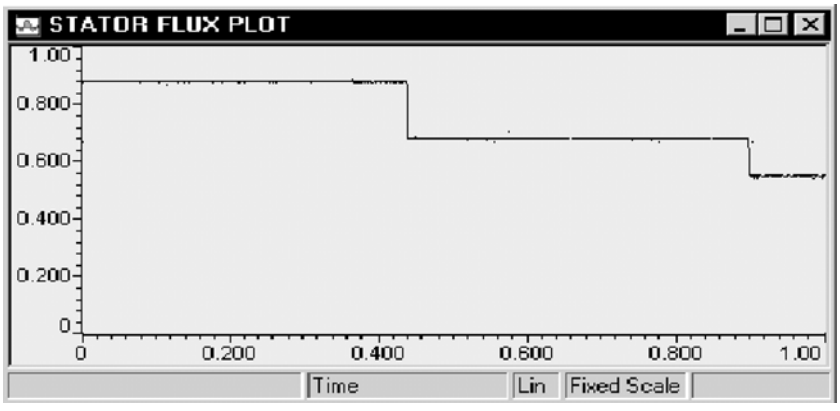

Fig. 13 Experimental results –Stator flux plot at the application of proposed algorithm of torque and flux ripple minimization at 600 rpm

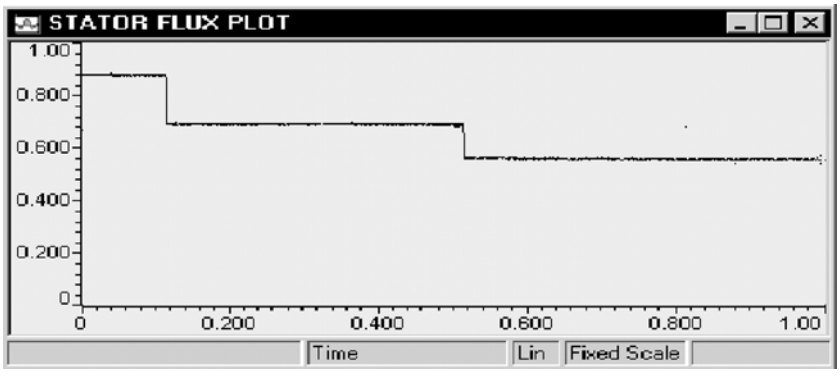

Fig. 14 Experimental results –Stator flux plot at the application of proposed algorithm of torque and flux ripple minimization at 100 rpm

using the proposed algorithm at different speeds such as 600 and 1000 rpm, respectively. From Fig. 11, it is observed that the torque pulsations are less using the proposed algorithm at 1000 rpm. When the proposed algorithm is applied, torque oscillates between 0.92 and 1 Nm. That is, the torque has no upper ripple and steady state torque reaches 1 Nm exactly. When compared to conventional DTC algorithm, percentage of torque ripple is much less when the proposed algorithm is applied. Generally, at low speed operation, torque ripple will be more when compared to high speed operations. But, using this proposed algorithm, this low speed torque ripple also reduced. These results show that the DTC scheme using the proposed algorithm has better torque response in terms of settling time and maximum overshoot. From the results, it is observed that the settling time is about 0.1 s. Magnitudes of stator flux plots through proposed algorithm are shown in Figs. 12, 13, and 14 at different speeds such as 1000, 600 and 100 rpm, respectively. Stator flux is weakened to 0.8 and 0.6 of the nominal value. Stator fluxes shown in these figures are in synchronously rotating frame. The fluxes appear as sinusoidal quantities in stationary frame. Locus of the stator flux with reduced ripple at 1000 rpm is shown in Fig. 15. This locus is obtained by considering the d-axis and q-axis fluxes in stationary frame. Usually, the stator flux and torque are

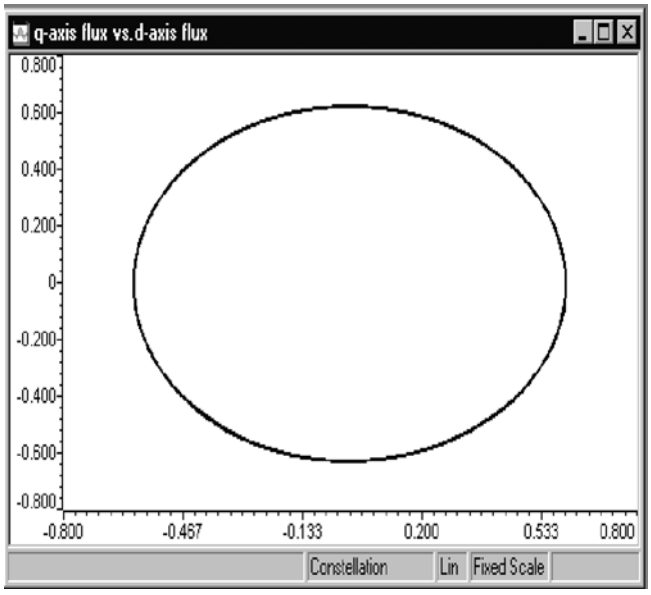

Fig. 15 Experimental results- Locus of stator flux with reduced ripple in DTC scheme using proposed algorithm at 1000 rpm

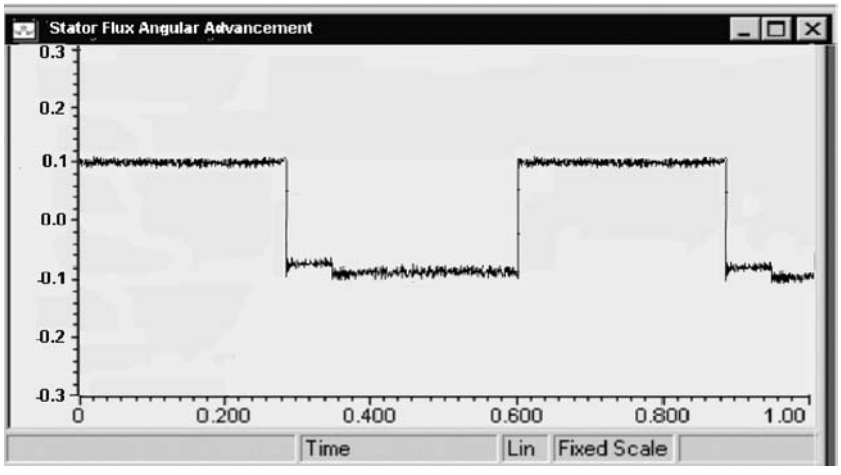

Fig. 16 Experimental results- Stator flux vector angular advancement at 1000 rpm

estimated using the mathematical expressions as given in Eqs. 1 and 5. In these calculations, stator resistance drop is also considered. DTC is less sensitive to parameter variations and less expensive than DFOC. However, at low speed operations, if switching frequency is not maintained constant, parameters of the motors are affected and the performance of the control will also be affected. This drawback of conventional DTC is overcome by the proposed algorithm of DTC in which the switching frequency is maintained constant. Figure 16 shows the angle of stator flux vector advancement at 1000 rpm. It can be seen that if the stator flux magnitude is decreased, the angle $\Delta\theta$ is raised to achieve demanded torque as given in Eq. 24. The value of $\Delta\theta$ is varied between $-\frac{\pi}{2} and \frac{\pi}{2}$ for various levels of stator flux. Steps 2 and 3 as given in Sect. 7 are applied to calculate $\Delta\theta$.

Experimental motor currents are shown in Fig. 17. From Fig. 17, it is observed that, the initial current seems to be high at the transient period. With reference to the stator flux, it can be noted that even a small variation of stator flux causes a large variation of the stator current. The transient portion of current is caused by a step variation of stator flux. At the starting point of steady state period, 3-phase stator current looks distorted. That is, some current ripple appear. However, by applying the proposed algorithm, this ripple is also reduced after 0.7 s. Table 1 shows the comparison of errors obtained in conventional DTC and DTC using the proposed algorithm with DFOC. The values shown in this table are index errors.

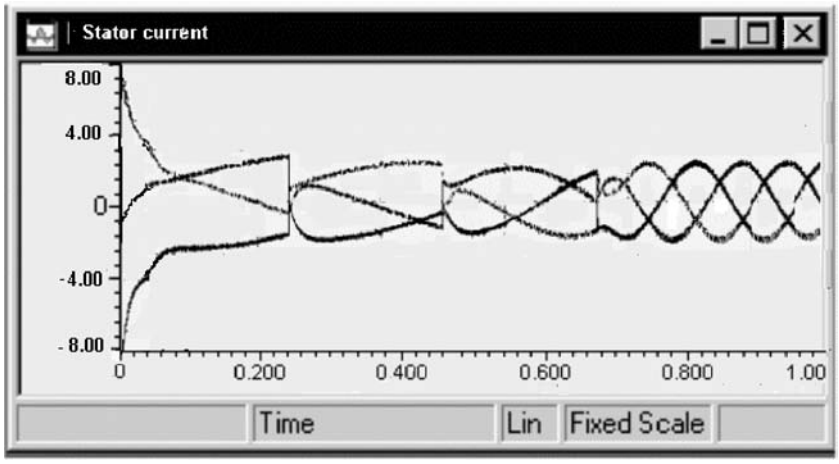

Fig. 17 Experimental results – 3- Phase stator currents of Induction motor at 1000 rpm

Table 1 Errors obtained in various control strategies

Sensorless DFOC		Conventional DTC		DTC using proposed algorithm	
Flux error	Torque error	Flux error	Torque error	Flux error	Torque error
2.53 e-3	0.189	2.2 e^{-3}	0.165	1.97 e-3	0.156
2.57 e-3	0.068	0.53 e^{-3}	0.025	0.48 e-3	0.023
7.46 e-3	0.0367	1.58 e^{-3}	0.0024	0.68 e-3	0.0010
2.46 e-3	0.297	2.1 e^{-3}	0.263	1.33 e-3	0.110

$e^{-3} = 10^{-3}$

9 Conclusion

This paper presents a novel direct torque and flux control algorithm for minimization of torque and flux ripple. This algorithm gives a unique solution for the voltage reference, which will drive torque and flux errors down to zero, by controlling both the radial and tangential component of stator flux vector increment. Proposed algorithm enables sensorless deadbeat control of torque and flux with constant switching frequency. Algorithm has no trigonometric functions and coordinate transformations compared to other solutions, and can be easily implemented on most recent digital controlled drives. Both simulation and experimental results prove the proposed algorithm.

Appendix

The rated values and parameters of the machine used in the simulation study and experiment are:

Po	Rated output power	1 H.P
V	Rated voltage	400 V
f_s	Rated frequency	50 Hz
P	Poles	4
N	Rated speed	1410 rpm
R_s	Stator resistance	10.4 Ω
R_r	Rotor resistance	11.6 Ω
L_s	Stator leakage inductance	22 mH
L_r	Rotor leakage inductance	22 mH
L_m	Mutual inductance	0.557 H
J	Moment of inertia	0.001 kg-m^2

References

1. Ohtani T, Takada N, Tanaka K (1992) Vector control of induction motor without shaft encoder. IEEE Trans Ind Appli 28:157–164
2. De Doneker R, Profumo F, Tenconi A (1993) The universal field oriented (UFO) controller in the air gap reference frame. J Inst Elect Eng D 113-D(4):477–486
3. Kwindler L, Moreira JC, Testa A, Lipo TA (1994) Direct field orientation controller using the stator phase voltage third harmonics. IEEE Trans Ind Appl 30:441–447
4. Vasudevan M, Arumugam R (2004) Different viable torque control schemes of induction motors for electric propulsion systems. Conf Rec IEEE Ind Appl soc II:2728–2737
5. Buja G, Casadei D, Serra G (2002) DTC – based strategies for induction motor drives. IEEE-IAS Annual Meeting, pp 1506–1516
6. Habetler TG, Profumo F, Pastorelli M, Tolbert LM (1992) Direct torque control of induction machines using space vector modulation. IEEE Trans Ind Appl 28(5):1045–1053
7. Griva G, Habetler TG (1995) Performance evaluation of a direct torque controlled drive in the continuous PWM-square wave transition region. IEEE Trans Power Electron 10(4):464- 471
8. Kenny BH, Lorenz RD (2003) Stator and rotor flux based deadbeat direct torque control of induction machines. IEEE Trans Ind Appl 39(4):1093–1101
9. Habetler TG, Profumo F, Pastorelli M (1992) Direct torque control of induction machines over a wide speed range. IEEE-IAS Annual Meeting, Conf Rec 1992, pp 600–606
10. Hurst KD, Habetler TG (1995) A simple, tacho-less, I. M. drive with direct torque control down to zero speed. IEEE Trans Ind Appl 5(5):563–568
11. Lascu C, Trzynadlowski A (2004) Combining the principles of sliding mode, direct torque control and space vector modulation in a high-performance sensorless AC drive. IEEE Trans Ind Appl 40(1):170–177
12. Habetler TG, Divan DM (1991) Control strategies for direct torque control using discrete pulse modulation. IEEE Trans Ind Appl 27(5):1064–1072

13. Isao T, Toshihiko N (1986) A new quick-response and high-efficiency control strategy of an induction motor. IEEE Trans Ind Appl IA-22(5):963–771
14. Depenbrock M (1988) Direct self-control (DSC) of inverter-fed induction machine. IEEE Trans Power Electron 3(4):445–453
15. Noguchi T, Yamamoto M, Kondo S, Takahashi I (1999) Enlarging switching frequency in direct torque–controlled inverter by means of dithering. IEEE Trans Ind App 35(6):675–684
16. Kang J-K, Sul S-K (1999) New direct torque control of induction motor for minimum torque ripple and constant switching frequency. IEEE Trans Ind Appl 35(5):1231–1239
17. Vas P (1998) Sensorless vector and direct torque control. Oxford University Press, London, pp 124–253
18. Buja GS, Kazmierkowski P (2004) Direct torque control of PWM inverter-fed AC motors – a survey. IEEE Trans IE 51